

Influence of L-cystine as an Additive in the Negative Electrolyte on Performance of Vanadium Redox Flow Battery

Nanfang Wang^{1,2,*}, Yong Chen¹, Huiguo Han¹, Min Cao¹, Xinqiang Bi¹, Sui Peng^{1,*}, Xingde Cheng¹

¹ Pangang Group Research Institute Co., Ltd., Panzhihua 617000, China

² School of Chemistry and Chemical Engineering, Hunan Institute of Engineering, Xiangtan 411104, China)

*E-mail: cdwnf@126.com (N. Wang), pengsui1976@yahoo.com.cn (S. Peng).

Received: 19 January 2017 / Accepted: 17 February 2017 / Published: 12 March 2017

L-cystine (LC) was employed as an additive to inhibit crystallization of V(II) or V(III) specie in the negative electrolyte and extend the practical application of vanadium redox flow battery (VRB) at below-ambient temperatures. UV-vis spectrometry showed LC has no effect on the absorption in the range of 300-800 nm. Crossover the membrane testing indicated that LC can permeate from Negative side to Positive side across the Nafion 117. Static thermal stability testing showed LC can significantly inhibit precipitation of V(II)~V(IV) ions or V(V) in 1.8 M vanadium electrolyte with 3.0 M H₂SO₄ at 5 or 50 °C. It is found that 2-4 wt% LC in vanadium electrolytes can lower viscosity compared to the blank electrolyte. Cyclic voltammetry (CV) and electrochemical impedance spectroscopy (EIS) show V(III) electrolyte with 2 wt% LC exhibits superior electrochemical activity and diffusion coefficient, compared with the pristine electrolyte. Introduction of LC into the negative electrolyte can obtain better performance of VRB with higher capacity retention (91.04% vs. 84.3%) and energy efficiency (75.77% vs. 72.27%) than the pristine electrolyte.

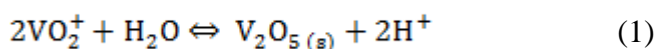
Keywords: Vanadium redox flow battery; L-cystine; Negative electrolyte; Thermal stability; Electrochemical activity

1. INTRODUCTION

Renewable energy sources like solar cells and wind turbines attract more and more attention owing to the critical issues of energy shortage and environment pollution caused by fossil energy resources [1]. However, the random and intermittent nature of renewable energy sources induces instability to the grid, which vastly limits their development. In order to smooth out the intermittency of renewable energy production, electrical energy storage (EES) has become indispensable for renewable energy to integrate into the grid. Compared to other batteries, Redox flow batteries (RFB)

are considered to be the best options for EES in the megawatt range [2]. Among these RFBs, vanadium redox flow battery (VRB) proposed by Skyllas-Kazacos and coworkers in 1980s [3, 4] is a better candidates for EES in the megawatt range, owing to its advantages such as no cross contamination of active species (vanadium element in both half-cells), better resistance to be over-charged and deeply-discharged, longer cycle life (more than 200,000 cycles), and lower operation and management cost (less than 0.001 \$/kWh) [5, 6]. Many megawatt demonstration systems have already been installed, for example, in Thailand, Japan, USA, and China [7].

The capacity and power output of VRB depend on the volume and concentration of the vanadium electrolytes. When the reservoir volumes of VRB system are defined, the concentration of the vanadium electrolyte will be vital to its energy density [8]. However, the high energy density of VRB (>25 Wh/kg [9]) is a challenge due to the poor solubility and stability of the vanadium species. The V(II), V(III), and V(IV) ions precipitate as sulfates, so their solubility increase with increasing temperature but decreases with increasing sulfuric acid concentration because of the common ion effect of the sulfate ion. On the other hand, V(V) electrolyte can undergo thermal precipitation to form V_2O_5 at elevated temperatures (>40 °C [9]) according to the endothermic reaction [10]:



So practical VRB systems operate with vanadium electrolyte concentration between 1.6 and 1.8 M and usually also employ electrolyte cooling and heating systems to maintain the temperature between 15 and 40 °C [11]. Therefore, a higher energy density flow battery electrolyte will allow a wider range of applications to be exploited.

Currently, the approaches to improve the solubility and stability of positive redox species are focused on optimization of the supporting acid electrolyte and utilization of stabilizing additives. A mixture acids (sulfuric/hydrochloric acid system [12, 13], sulfuric/methane sulfonic acid [14], sulfuric/sulfamic acid [15]) as supporting electrolyte can considerably improve the thermal stability of V(V) ions. The use of sulfuric/hydrochloric acid system introduces the risk of acid, chlorine vapor at high temperatures or during overcharge presenting a potential safety hazard. Both Methane acid and sulfamic acid can greatly increase the cost of VRB. A efficient way to inhibit the precipitation of V(V) ions is addition of stabilizing agent in vanadium electrolyte [16, 17]. Some typical organic additives with oxygen and nitrogen functional groups, such as D-sorbitol [18], L-glutamic acid [19], pyridine carboxylic acid [20], and coulter dispersant [21], are effective in inhibiting the formation of V(V) ion precipitants at elevated temperature, moreover, they can improve the electrochemical performance of the VRFB.

So far, additives for the positive electrolyte of VRB have been investigated intensively to improve its stability and electrochemical activity, but there is few researches to investigate whether these additives would have positive influences on the properties of negative electrolyte. Liu, J., et al. [22] used DL-malic acid and L-aspartic acid as additives for the negative electrolyte of VRB. The introduction of L-aspartic acid into the 2 M V(III) electrolyte can stabilize the electrolyte by delaying its precipitation, increase the diffusion coefficient of V(III) species, and facilitate the charge transfer of V(III)/V(II) redox reaction. Li, X., et al. [23] investigated several compounds (Oxalic acid, Ammonium oxalate, Ethylene diamine tetraacetic acid, Glucose, D-fructose, and α -lactose) as

additives of V(III) electrolyte. The results showed that a small amount of additives can improve solubility and stability of V(III) ion in H₂SO₄ solution. Charge/discharge test indicated VRB with 1.8 M V(III) electrolyte containing 1 wt% Oxalic acid as catholyte had a higher unit volume capacity. Guan, T., et al. [24] adopted five additives for VRB's negative electrolyte. The experiments showed urea, ammonium oxalate and ethylene glycol can inhibit the crystallization of the V(III) ions while magnesium sulfate and sodium sulfate have no effects on the V(III) crystallization. The voltage efficiency (VE) and coulombic efficiency (CE) of the battery were significantly increased for urea and ammonium oxalate additives. These results show some compounds containing -NH₂, -OH, etc. groups can inhibit the crystallization of the V(III) ions and improve its diffusion coefficient and electrochemical activity.

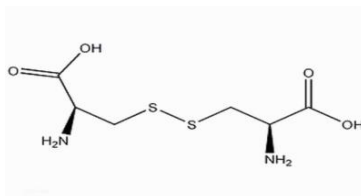
In the practical VRB system with additives in positive electrolyte, capacity decay during charge-discharge cycles is observed, due to the accumulation of vanadium ions on one side of the cell and dilute to the other caused by the differential diffusion of vanadium ions across the membrane [25]. Such a loss of the capacity can usually be regenerated by simply remixing the two half-cell solutions. Influence of the organic additive on the negative electrolyte is essential to the performance of VRB, especially in lower temperature conditions [22, 26], which is helpful to extend the practical application of VRB in the large-scale energy storage.

L-cystine (LC) is a specific amino acid containing functional groups (-OH, -NH₂, -S-) (Scheme 1) and commonly used as an additive for nutrition and cosmetic. In this paper, LC is adopted as a negative electrolyte additive due to its unique structure. The effects of LC on the precipitation behaviour at 5 °C and electrochemical performance of V(III) electrolyte for VRFB are examined.

2. EXPERIMENTAL

2.1 Preparation of vanadium electrolyte

In this work, the original 1.8 M vanadium electrolyte containing with 3.0 M H₂SO₄ was prepared by electrolytic dissolution and reduction of V₂O₅ (99.93%, Pangan Group Co., Ltd.) in sulfuric acid (99.95%, Chengdu Kelong chemical reagent factory) in a two-compartment electrolysis cell [22]. The chemical composition of V₂O₅ measured by ICP was listed in Table 1. The total content of impure metal elements is less than 0.07% and Na represents 0.0047%. The termination of electrolysis was determined by a UV-vis measurement. The characteristic absorption peak of V(IV) appears at 770 nm and those of V(III) appear at 401.0 nm and 606.5 nm, respectively. The concentration of vanadium was analyzed by redox titration. The electrolyte samples with LC were prepared by adding 1 to 4 wt% LC (99.5%, Chengdu Kelong chemical reagent factory) to the prepared pristine electrolyte. The chemical structure of LC is shown in Scheme 1.



Scheme 1. Chemical structure of L-cystine.

Table 1. Chemical composition of V_2O_5 measured by ICP.

Element	Al	As	Ca	Co	Cr	Cu	Fe	Mg	K	Mn
Content (wt %)	0.0010	0.0011	0.0091	0.0003	0.0026	0.0004	0.0135	0.0010	0.0159	0.0009
Element	Mo	Na	Ni	P	Si	Ti	Pb	Zn	V_2O_5	
Content (wt %)	-	0.0047	0.0010	0.0010	0.0163	0.0021	0.0010	0.0002	99.9279	

2.2 Static thermal stability of vanadium electrolyte

Thermal stability test of V(II), V(III), and V(IV) electrolyte was carried out by monitoring and recording the induction time for vanadium precipitates statically placed at low temperature. In a typical procedure for thermal stability test, 20 mL 1.8 M V(III) electrolyte solution by adding a certain amount of LC was injected into an airtight tube. Then the tube was statically stored in a temperature-controlled container (GDJS-100, Wuxi Yishun Testing equipment Co., Ltd.) at 5 °C. The induction time was recorded at regular intervals until a visible precipitate appeared in the tube. As for V(V) electrolyte, the testing temperature was set at 50 °C. Testing results were given as the arithmetic means of three replicated experiment samples, unless otherwise stated.

2.3 Redissolution of vanadium precipitates with agitation

The sample tubes with precipitates were fitted on a vibrator (SHA-C, Ningbo Testing Equipment Co., Ltd.) stored in the temperature-controlled container (GDJS-100) at 5 °C and agitated at 200 rpm for 4 h to see if the precipitates could dissolve again.

2.4 Kinematic viscosity of electrolyte solution

Kinematic viscosity (mm^2/s) of each vanadium electrolyte solution at 5 °C was determined by a viscosity meter (SYD-265B, Shanghai Testing Equipment Co., Ltd.) and a 0.8 mm capillary tube with the viscosity constant of $0.07873 \text{ mm}^2/\text{s}^2$ was adopted. For V(II) electrolyte measurement, N_2 gas was used for avoiding oxidation. The viscosity results were obtained according to the following equation,

$$\eta = c \cdot \tau \quad (2)$$

where c denotes viscosity constant of $0.07873 \text{ mm}^2/\text{s}^2$, and τ denotes the mean value for three flowing times.

2.5 Ultraviolet-visible spectroscopy

Ultraviolet-visible (UV-vis) spectroscopy of V(III) electrolyte was measured on the UV/vis spectrophotometer (TU-1901, Shanghai) in the range of 200-800 nm using 10 mm path-length quartz cell. The measured solutions were 0.04 M V(III) electrolyte in 3.0 M H₂SO₄ with and without 2 wt% LC. A solution of 3.0 M H₂SO₄ was used as the reference solution.

2.6 Cyclic voltammetry (CV)

CV was measured on an Autolab electrochemical workstation (Metrohm, Swiss) at a scan rate of 5-200 mV·s⁻¹ between -0.8 V and 0.0 V at room temperature. A three-electrode system was used with Pt plate (2.0×2.0 cm²) as counter electrode, a saturated calomel electrode (SCE) as reference electrode, and a graphite electrode with a surface area of 1.0×1.0 cm² as working electrode. The graphite electrode was polished with 600 (P1200) grit SiC paper, then cleaned with de-ionized water. To avoid cross-contamination of different ions on the electrode surface, the graphite electrode was polished and rinsed carefully after each test.

2.7 Electrochemical impedance spectroscopy(EIS)

EIS was performed with an Autolab electrochemical workstation (Metrohm, Swiss) at room temperature. The sinusoidal excitation voltage applied to the cells was 5 mV with a frequency range between 0.01 Hz and 100.0 kHz.

2.8 Crossover the membrane for LC

The permeability of LC through Nafion 117 membrane was measured using a membrane-separated diffusion cell [27]. At room temperature, 40 ml solution of 2 wt% LC in 3.0 M H₂SO₄ (Negative side) and 40 mL solution of 3.0 M H₂SO₄ (Positive side) were statically placed in opposing reservoirs separated by the membrane for 24 h. Two aliquots from the Negative side and the Positive side were taken and analyzed for LC by a UV-vis spectrometer (TU-1901) with a 3.0 M H₂SO₄ solution as the blank reference.

2.9 Cell test

A VRB single cell was fabricated by sandwiching the membrane (Nafion 117, Dupont Co., Ltd.) between two pieces of graphite felt (thickness is 5 mm, Shenhe carbon fiber Materials Co., Ltd.) with effective reaction area of 30 cm², which was served as the electrodes, and conductive plastic (thickness is 0.4 mm and resistivity is 0.2 ohm·cm, Pangang Group Co., Ltd.) were used as the current collectors. 100 mL 1.8 M V(IV) in 3.0 M H₂SO₄ serving as positive electrolyte and 100 mL 1.8 M V(III) in 3.0 M H₂SO₄ with 2.0 wt% L-cystine additive as negative electrolyte were cyclically pumped into the corresponding half-cell respectively. The single cell was charged and discharged by a

CT2001C-10V/10A battery test system (Wuhan Land Co., Ltd.) with a constant current density of 60 mAcm^{-2} at room temperature. To avoid the corrosion of the carbon felt electrodes and conductive plastic, the upper limit of charge voltage was 1.7 V and the lower limit of discharge voltage was 0.7 V.

3. RESULTS AND DISCUSSION

3.1 UV-Vis spectrometry

The UV-Vis spectra for V(III) electrolyte with and without 2 wt% LC as additive are shown in Fig. 1. The characteristic absorption peaks for V(III) ions appear at approximately 401 nm and 606.5 nm, respectively. Compared with the pristine V(III) electrolyte, there is neither new absorption peak nor wavelength shift for the electrolyte with 2 wt% LC. This indicates that LC additive has no effect on the valence state as well as the effective concentration of vanadium ions.

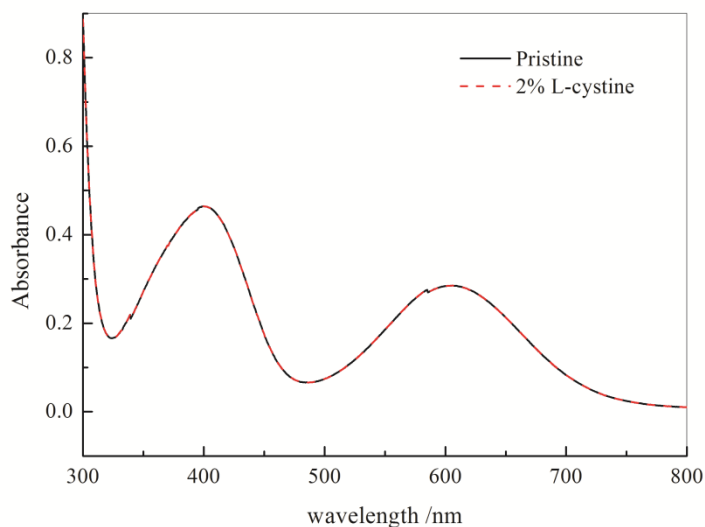


Figure 1. The UV-Vis spectra for 0.04 M V(III) electrolyte with and without 2% LC additive.

3.2 Crossover the membrane for LC

The diffusion of L-cystine across the membrane is an interesting topic to explore. Fig. 2 shows UV-Vis spectra for LC in the Negative side and Positive, indicating that LC can permeate from Negative side to Positive side across the membrane Nafion 117. There is no absorption peak over the wavelength range of 400-700 nm for LC, but the maximum absorption peak at the range of 240-250 nm. Therefore, UV-Vis spectra can be used for detecting LC in the Positive side solution. This crossover strengthens the necessity of studying the effect of additive on positive electrolyte.

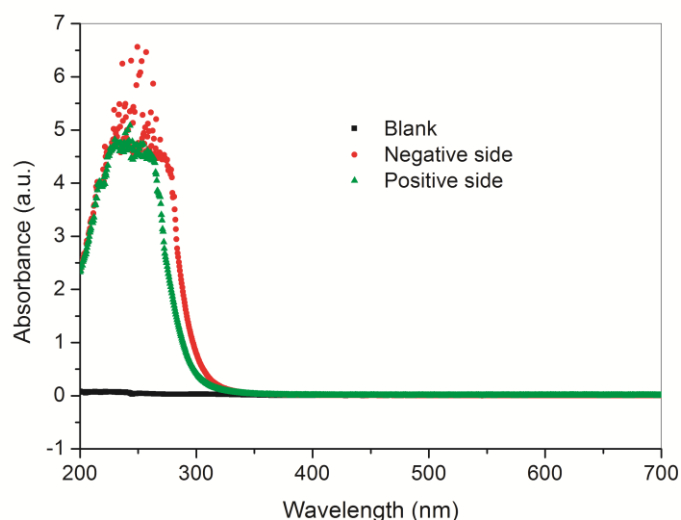


Figure 2. UV-Vis spectra for LC in the Negative side and Positive side.

3.3 Effects of LC on the thermal stability and viscosity of vanadium electrolyte

The induction time of precipitation for the vanadium solution (1.8M) with LC additive is presented in Table 2. For the samples with 3M sulfur acid at 5 °C, it can be found that the induction time of V(III) electrolyte with LC is longer than that of the pristine sample. The induction time gradually increases with LC amount. The addition of 4 wt% LC can delay the precipitation of V(III) species for 386 h at 5 °C. For 4M sulfur acid, the induction time of the pristine sample is 52 h while that of 2 wt% L-cystine sample is 81 h. This indicates that L-cystine can effectively increase the thermal stability of V(III) ions. In the same way, LC can also increase the induce time of precipitation of V(II) and V(IV) at low temperature, compared to the pristine sample. As for V(V) and 90% V(V)+10% V(IV) (SOC=90%), LC can retard the precipitation at high temperature. Both V(II) and V(III) ions are hydrated with 6H₂O, and exist in the form of [V(H₂O)₆]²⁺ and [V(H₂O)₆]³⁺, forming an octahedral structure. For V(IV) ions, ¹H and ¹⁷O NMR spectra showed there is weakly electrostatic interaction between sulphate anions and [VO(H₂O)₅]²⁺ to form the second-coordination sphere [28]. H₂O molecule is a weak ligand. Increasing sulphuric acid concentration or decreasing temperature, structures of V(II), V(III), and V(IV) hydrated ions will inevitably be destroyed, and they come into crystal nucleation and growth and precipitation. In our study, L-cystine was adopted as negative electrolyte additive due to its multi-functional groups (-OH, -NH₂, and -s-), which have stronger coordination to V(II) and V(III) ions than H₂O molecule. This more stable coordination will prevent or delay the vanadium precipitation. On the other hand, NH₂ group of L-cystine can absorb H⁺ in the strong acid media and thus V(LC)³⁺ possesses higher electrostatic repulsion. Therefore, it is considered that steric hindrance and electrostatic repulsion are the main stabilizing mechanism for L-cystine and vanadium species. This result is consistent with the report by Liu et al. [22].

Table 2 shows viscosity values of vanadium electrolyte with L-cystine are lower than that of the pristine sample, which facilitates flow and distribution of the electrolyte solution in the graphite

felt electrode. Introduction of L-cystine into vanadium electrolyte can improve its dispersion and lower its viscosity due to the formation of $V(LC)^{3+}$.

Table 2 indicates the effect of mechanical agitation on redissolution of vanadium precipitates from the static experiment. All the precipitates of V(II), V(IV), V(IV) species samples with LC can dissolve again with agitation without heating. In comparison, All the precipitates of V(II), V(IV), V(IV) species pristine samples can not redissolve completely, but can dissolve away when heating. This difference is attributed to the different precipitate structures between the pristine and LC samples. The precipitates from pristine samples of V(V) and 90% V(V)+10%V(IV) can be insoluble with agitation when cooling due to the irreversible process in Eq. (1).

Table 2. Induction time and viscosity of 1.8M vanadium electrolyte with LC and redissolution of its precipitate.

V species	Temperature / °C.	Sulfuric acid / M	LC / wt%	Time / h	Viscosity / mm ² /s	Redissolution phenomena
V(III)	5	3	0	324	8.41	+ -
		3	1	330	8.28	+
		3	2	342	8.15	+
		3	3	360	7.96	+
		3	4	386	7.74	+
		4	0	52	8.66	+ -
		4	2	81	8.48	+
V(II)	5	3	0	260	6.34	+ -
		3	2	320	6.08	+
V(IV)	5	3	0	208	7.12	+ -
		3	2	312	6.36	+
V(V)	50	3	0	48	6.30	-
			2	NF	6.07	
90% V(V)+10% V(IV)			0	128	6.49	-
			2	NF	6.11	

Note: NF represents found precipitate. (+) Soluble; (+ -) Soluble when heating; (-) insoluble.

3.4 CV

Cyclic voltammetry technique is adopted to investigate the effect of LC on the redox reaction of negative electrolyte in VRB. It is more appropriate using a glassy carbon as working electrode in CV study of VRB electrolyte. But the graphite electrode is commonly used in the vanadium electrolyte CV test [29, 30]. So we used the graphite plate as working electrode and obtained the CV results in accordance with those by the glassy carbon electrode [31, 32]. The CV curves of 1.8 M V(III) in 3 M H₂SO₄ without and with 1-4 wt% LC additive at the scan rate of 20 mVs⁻¹ between -0.8 V and 0.0 V are shown in Fig. 3. The anodic and cathodic peaks of the V(III)/V(II) redox reaction are observed at approximately -0.45 V and -0.65 V, respectively. The addition of LC can increase both oxidation peak

current and reduction peak current suggesting that adding LC can enhance the electrochemical activity. The reduction of the anodic to cathodic peak separation indicates better electrochemical reversibility of the V(III)/V(II) redox reaction in the electrolyte with LC. Main related parameters related to CV are presented in Table 3 for comparison. With LC, the anodic peak current as well as cathodic peak current increases and then decreases. Meanwhile the anodic to cathodic peak separation (ΔE_p) and the peak current ratio of cathodic peak to anodic (j_{pc}/j_{pa}) decrease and then increase. At 2 wt% LC addition, the cathodic and anodic peak currents reach a maximum, and rise by 16.61% and 8.20% respectively, compared to the pristine electrolyte. The peak current ratio of cathodic peak to anodic (j_{pc}/j_{pa}) reaches a minimum of 1.10. This result indicates the negative vanadium electrolyte with 2 wt% LC has the optimal electrochemical activity and electrochemical reversibility. This is due to the fact that functional groups (e.g. C=O-OH, -NH₂, -S-) on the L-cystine can be absorbed on the electrode, which will be conducive to the V(II)/V(III) redox reaction [22].

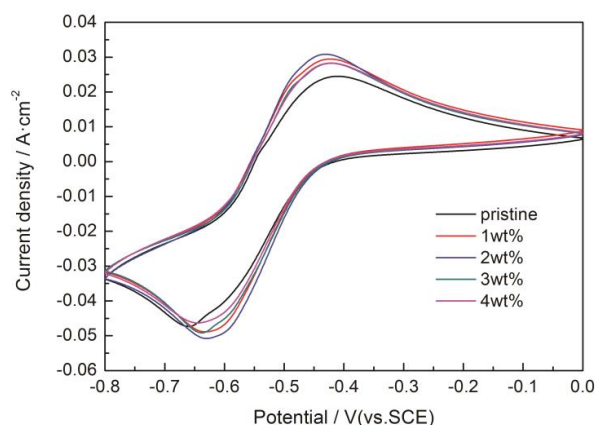


Figure 3. CV of the negative electrolyte with various amount of LC at 20 mVs⁻¹.

Table 3. CV data for V(III) electrolyte with various amount of LC at 20 mVs⁻¹.

Sample	Anodic peak		Cathodic peak		$\Delta E_p/V$	j_{pc}/j_{pa}
	$j_{pa}/\text{mA cm}^{-2}$	E_{pa}/V	$j_{pc}/\text{mA cm}^{-2}$	E_{pc}/V		
Pristine	39.49	-0.406	46.93	-0.661	0.255	1.19
1 wt%	43.46	-0.422	48.87	-0.631	0.209	1.12
2 wt%	46.05	-0.432	50.78	-0.629	0.197	1.10
3 wt%	43.26	-0.422	49.15	-0.637	0.215	1.14
4 wt%	40.31	-0.422	46.31	-0.648	0.226	1.15

In order to further investigate the effect of the additive on the kinetics of V(II)/V(III) redox reaction, CV curves of 1.8 M V(III) electrolyte without and with 2 wt% LC at scan rates from 5 to 200 mVs⁻¹ are shown in Fig. 4. The peak current increases in linear with the augment of scan rate, and all the peak potential intervals (ΔE_p) are larger than 59 mV, which indicates that the V(II)/V(III) redox

reaction is quasi-reversible. As for the quasi-reversible reaction, the diffusion coefficient D_o of V(III) ions is calculated according to the following procedure. Firstly, the redox reaction of V(II)/V(III) is assumed as a reversible reaction to calculate the D_o according to eq. (3). The rate constant k can be calculated according to eq. (5).

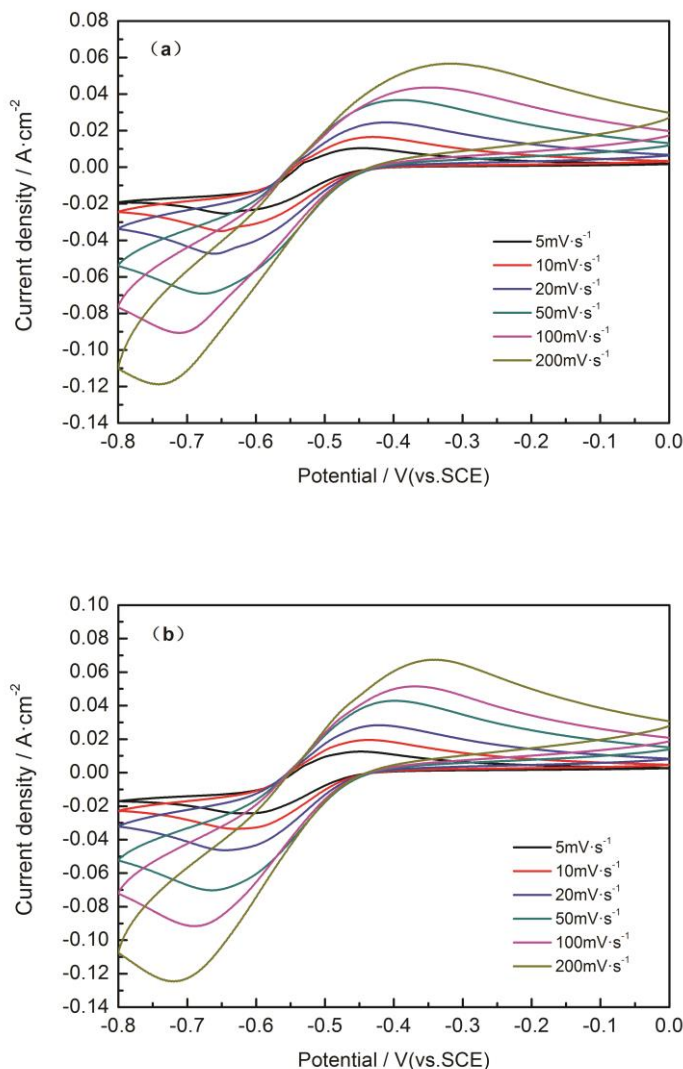


Figure 4. CV with scan rates from 5 to 200 mVs⁻¹ for (a) pristine sample and (b) 2 wt% LC sample.

Secondly, use k and D_o to verify if the reaction is reversible, quasi-reversible, or irreversible [33]. Thirdly, choose appropriate equation for calculation of D_o .

For the reversible reaction,

$$i_p = 2.69 \times 10^5 n^{3/2} A C D_o^{1/2} v^{1/2} \quad (3)$$

For the irreversible reaction,

$$i_p = 2.99 \times 10^5 n^{3/2} a^{1/2} A C D_o^{1/2} v^{1/2} \quad (4)$$

For the quasi-reversible reaction,

$$\psi = \Lambda \pi^{-1/2} = \frac{(D_o/D_R)^{a/2} k^0}{(\pi D_o f v)^{1/2}} \tag{5}$$

where i_p is the peak current, n is the number of electrons involved in the electrode reaction, a is the charge transfer coefficient ($a \approx 0.5$), A is the electrode area, C is the concentration of active species, D_o is the diffusion coefficient, v is the scan rate.

In eq. (5), ψ is the equivalent parameter, Λ is the quantitative measure of reversibility, D_o is the diffusion coefficient of V(III), D_R is the diffusion coefficient of V(II), k^0 is the rate of the redox reaction, f is a constant of nF/RT . Assuming $D_o = D_R$ and $a \approx 0.5$, eq. (5) can be changed into the following equation.

$$\psi = \Lambda \pi^{-1/2} = \frac{k^0}{(\pi D_o f v)^{1/2}} \tag{6}$$

According to the eq. (3), D_o is $3.78 \times 10^{-7} \text{ cm}^2 \cdot \text{s}^{-1}$ and $2.62 \times 10^{-7} \text{ cm}^2 \cdot \text{s}^{-1}$ for 2 wt% LC sample and pristine sample, respectively, by using the linear fitting of the relationship between i_p and $v^{1/2}$, shown as in Fig. 5. According to the variation of ΔE_p with ψ [33], the range of k^0 is calculated as $1.23 \times 10^{-4} v^{1/2} - 1.85 \times 10^{-3} v^{1/2} \text{ cm} \cdot \text{s}^{-1}$ for 2 wt% LC sample, and $5.19 \times 10^{-5} v^{1/2} - 9.34 \times 10^{-4} v^{1/2} \text{ cm} \cdot \text{s}^{-1}$ for pristine sample, respectively. Therefore, for both the pristine and LC sample, it is a quasi-reversible reaction at scan rates from 5 to 200 mVs^{-1} . D_o for a quasi-reversible reaction is recalculated using eq. (6) and listed in Table 4. It is obvious that the diffusion coefficient of LC sample is higher than that of the pristine sample, indicating that LC can facilitate the mass transport and improve the electrochemical activity of negative vanadium ions due to the lower viscosity and the coordination between V(III) ions and L-cystine (V(LC)^{3+}).

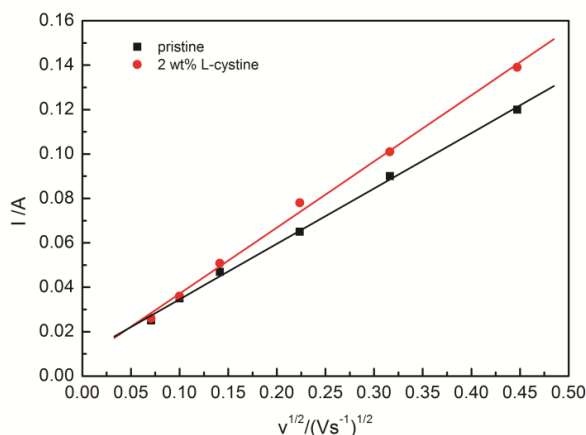


Figure 5. Linear fitting for the relationship between i_p and $v^{1/2}$.

Table 4. Diffusion coefficients of V(III) electrolytes with or without LC.

Diffusion coefficient	Reaction	Pristine	2 wt% L-cystine
D_o ($10^{-7} \text{ cm}^2 \cdot \text{s}^{-1}$)	reversible	2.63	3.78
D_o ($10^{-7} \text{ cm}^2 \cdot \text{s}^{-1}$)	irreversible	4.25	6.12
D_o ($10^{-7} \text{ cm}^2 \cdot \text{s}^{-1}$)	quasi-reversible	2.39	3.93

3.5 EIS

Electrochemical impedance spectroscopy (EIS) was applied to further analyze the effect of LC on the electrochemical performance of V(III) electrolyte and the Nyquist plots are shown in Fig. 6. A single depressed semicircle in the high frequency region and a straight line in the low frequency region can be observed in each plot, demonstrating that the V(III)/V(II) redox reaction should be mix-controlled by electrochemical reaction and diffusion steps. The radius of the semicircle corresponds to the charge transfer resistance, while the linear part is associated with the diffusion of vanadium species in the electrode [34]. A simplified equivalent circuit is proposed in Fig. 6, where R1 consists of the electrolyte resistance and electrode resistance, C represents the electric double-layer capacitance of electrode/electrolyte interface, Q is the constant-phase element representing the diffusion capacitance caused by the diffusion process of vanadium ions in the electrode, and R_{ct} stands for the charge transfer resistance [35]. The EIS results are obtained by fitting the plots with the equivalent circuit, as presented in Table 5. It can be seen that the contact resistance R₁ slightly decreases in the electrolyte with 2 wt% L-cystine. Moreover, R_{ct} of the electrolyte with L-cystine is 4.67 ohm cm⁻², much lower than that of the pristine electrolyte. The reduced R_{ct} implies faster charge transfer process, which might be due to the catalytic property of absorbed oxygen and nitrogen groups on the electrode [22]. Besides, the hydrophilic nature of the groups favors the absorption and diffusion of vanadium species, which can be responsible for the increase of the electric double-layer capacitance of electrode/electrolyte interface and the diffusion capacitance of ions.

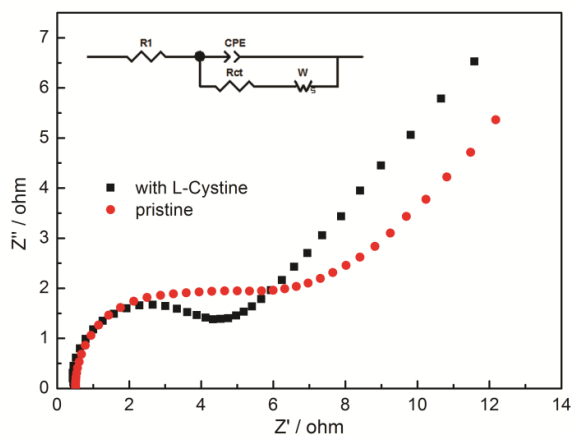


Figure 6. Nyquist plots of the negative electrolyte with or without LC and the corresponding equivalent circuit.

Table 5. Fitting results of EIS.

Sample	R ₁ (Ω cm ⁻²)	CPE		R _{ct} (Ω cm ⁻²)
		Y ₀ Ω ⁻¹ s ⁿ	n	
Pristine	0.51	4.6×10 ⁻⁵	0.78	7.26
2 wt% LC	0.50	1.1×10 ⁻⁴	0.90	4.67

3.6 Cell test

Fig. 7 presents the typical charge-discharge curves of cells using negative electrolyte with and without LC. The cell with LC in the electrolyte exhibits higher capacity and smaller interval between charge and discharge plateau, indicating the improvement of electrochemical reversibility and activity, which is consistent with the CV and EIS results.

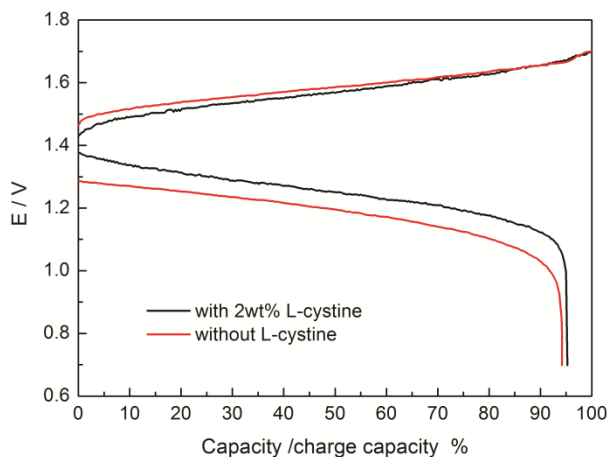


Figure 7. Charge-discharge curves of cell employing negative electrolyte with or without LC.

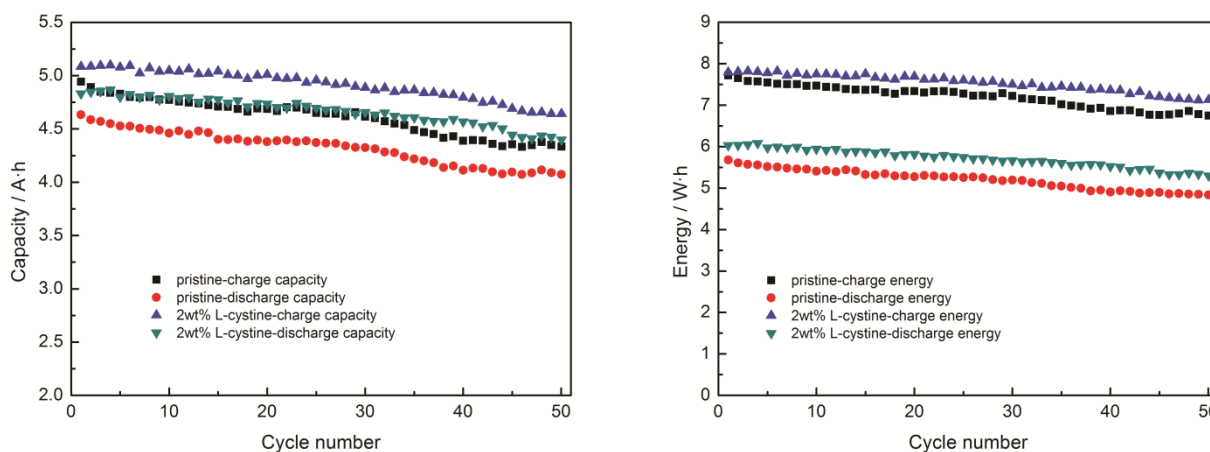


Figure 8. Capacity and energy of cell employing negative electrolyte with or without LC.

The capacity and energy of the cells in 50 cycles are compared in Fig. 8. The 1st capacity and energy of the cell with LC electrolyte sample are 4.831 Ah and 6.03 Wh, respectively, higher by 0.197 A h and 0.35 W h than those with the pristine. The 50th capacity and energy of the cell with LC electrolyte sample are 4.398 A h and 5.29 W h, respectively, higher by 0.325 A h and 0.46 W h than those with the pristine. This result indicates LC can increase the utility ratio of active species and restrain the capacity and energy decay. The improvement in capacity and energy retention (91.04%

and 87.33%) is probably attributed to less vanadium ion crossover or decreased electrolyte/valance imbalance resulting from the formation of $V(LC)^{3+}$. Moreover, cycling data in Fig. 8 indicate the additive LC has no effect on the conductivity and selectivity of the membrane over long-term operation [36].

Coulombic efficiency (CE) and energy efficiency (EE) of the cells employing negative electrolyte with and without LC in 50 cycles is shown in Fig. 9. Introduction of LC elevates the average CE from 93.86% to 94.97%. The average EE of the cell with LC in the electrolyte is 75.77%, 3.5% higher than that of the pristine one, demonstrating the enhancement of electrochemical performance. The excellent electrochemical performance of the cell with LC in the electrolyte should be ascribed to its functional groups of $-COOH$, $-NH_2$, and $-S-$.

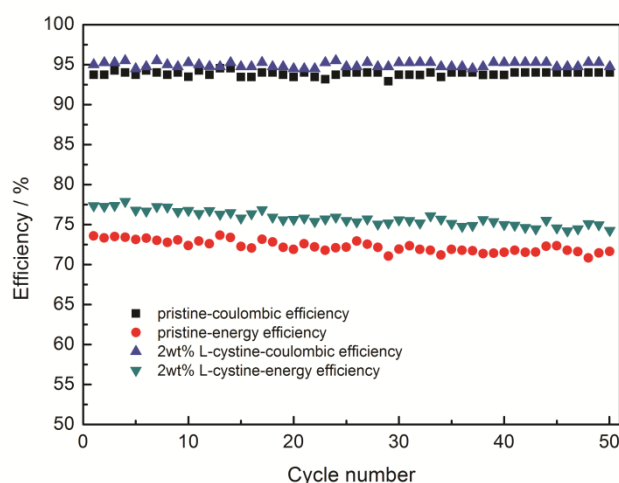


Figure 9. Coulombic efficiency and energy efficiency of cell employing negative electrolyte with or without LC.

4. CONCLUSIONS

LC has no effect on the UV-vis spectrometry of $V(III)$ electrolyte solution and can permeate from Negative side to Positive side across the membrane. The addition of LC can significantly increase thermal stabilities at 5-50 °C and decrease viscosities of $V(II)$ ~ $V(V)$ electrolyte solutions. CV and EIS tests showed that the electrochemical activity and reversibility of $V(II)/V(III)$ redox reaction have been improved greatly by LC additive. The improvement might be attributed to the formation of $V(LC)^{3+}$ facilitating lower mass transfer resistance and higher activity of redox reaction. The VRB using negative electrolyte containing LC shows excellent charge-discharge performance with capacity retention of 91.04% and average energy efficiency of 75.77% in 50 cycles. Therefore, L-cystine can be considered as a promising additive for negative electrolyte of VRB helpful to extend the practical application of VRB in the large-scale energy storage.

ACKNOWLEDGEMENTS

This work was financially supported by the Scientific Research Fund for the Application Project of Pangan Group (2014P4C9C01Z) and the Doctoral Scholars of Hunan Institute Engineering (13094).

References

1. M. Skyllas-Kazacos, L. Cao, M. Kazacos, N. Kausar, A. Mousa, *ChemSusChem* 9 (2016) 1521.
2. C. Ponce de Leona, A. Frias-Ferrer, J. Gonzalez-Garciab, D.A. Szantoc, F.C. Walsh, *J. Power Sources* 160 (2006) 716.
3. M. Skyllas-Kazacos, M. Rychcik, R.G. Robins, A.G. Fane, M.A. Green, *J. Electrochem. Soc.* 133 (1986) 1057.
4. M. Skyllas-Kazacos, F. Grossmith, *J. Electrochem. Soc.* 134 (1987) 2950.
5. M. Ulaganathan, V. Aravindan, Q. Yan, S. Madhavi, M. Skyllas-Kazacos, T.M. Lim, *Adv. Mater. Interface.* 3 (2016) 1500309.
6. P. Leung, X. Li, C. Ponce de Leon, L. Berlouis, C.T.J. Low, F.C. Walsh, *RSC Adv.* 2 (2012) 10125.
7. X. Li, H. Zhang, Z. Mai, H. Zhang, I. Vankelecom, *Energ. Environ. Sci.* 4 (2011) 1147.
8. S. Peng, N. Wang, X. Wu, S. Liu, D. Fang, Y. Liu, K. Huang, *Int. J. Electrochem. Sci.* 7 (2012) 643.
9. M. Skyllas-Kazacos, C. Menictas, M. Kazacos, *J. Electrochem. Soc.* 143 (1996) L86.
10. F. Rahman, M. Skyllas-Kazacos, *J. Power Sources* 72 (1998) 105.
11. M. Skyllas-Kazacos, G. Kazacos, G. Poon, H. Verseema, *Int. J. Energ. Res.* 34 (2010) 182.
12. M. Vijayakumar, W. Wang, Z. Nie, V. Sprenkle, J. Hu, *J. Power Sources* 241 (2013) 173.
13. L. Li, S. Kim, W. Wang, M. Vijayakumar, Z. Nie, B. Chen, J. Zhang, G. Xia, J. Hu, G. Graff, J. Liu, Z. Yang, *Adv. Energ. Mater.* 1 (2011) 394.
14. S. Peng, N.f. Wang, X.J. Wu, S. Liu, D. Fang, Y.n. Liu, K.l. Huang, *Int. J. Electrochem. Sci.* 7 (2012) 643.
15. Z. He, Y. He, C. Chen, S. Yang, J. Liu, Z. He, S. Liu, *Ionics* 20 (2014) 949.
16. S. Peng, N. Wang, C. Gao, Y. Lei, X. Liang, S. Liu, Y. Liu, S. Peng, N. Wang, C. Gao, *Int. J. Electrochem. Sci.* 7 (2012) 2440.
17. S. Peng, N. Wang, C. Gao, Y. Lei, X. Liang, S. Liu, Y. Liu, *Int. J. Electrochem. Sci.* 7 (2012) 4388.
18. S. Li, K. Huang, S. Liu, D. Fang, X. Wu, D. Lu, T. Wu, *Electrochim. Acta* 56 (2011) 5483.
19. X. Liang, S. Peng, Y. Lei, C. Gao, N. Wang, S. Liu, D. Fang, *Electrochim. Acta* 95 (2013) 80.
20. H. Han, Z. He, J. Liu, Y. Chen, S. Liu, *Ionics* 21 (2014) 167.
21. F. Chang, C. Hu, X. Liu, L. Liu, J. Zhang, *Electrochim. Acta* 60 (2012) 334.
22. J. Liu, S. Liu, Z. He, H. Han, Y. Chen, *Electrochim. Acta* 130 (2014) 314.
23. X. Li, X.L. Xie, Yafei, *J. Chem. Ind. Eng. (China)* (2011) 140.
24. T. Guan, M. Lin, Q. Yu, *Battery Bimonthly* 41 (2011) 37.
25. D.H. Hyeon, J.H. Chun, C.H. Lee, H.C. Jung, S.H. Kim, *Korean J. Chem. Eng.* 32 (2015) 1554.
26. A. Mousa, M. Skyllas-Kazacos, *ChemElectroChem* 2 (2015) 1742.
27. N. Wang, S. Peng, D. Lu, S. Liu, Y. Liu, K. Huang, *J. Solid State Electr.* 16 (2012) 1577.
28. M. Vijayakumar, S.D. Burton, C. Huang, L. Li, Z. Yang, G.L. Graff, J. Liu, J. Hu, M. Skyllas-Kazacos, *J. Power Sources* 195 (2010) 7709.
29. J. Shen, S. Liu, Z. He, L. Shi, *Electrochim. Acta* 151 (2015) 297.
30. G. Wang, J. Chen, X. Wang, J. Tian, H. Kang, X. Zhu, Y. Zhang, X. Liu, R. Wang, *J. Energy Chem.* 23 (2014) 73.
31. E. Sum, M. Skyllas-Kazacos, *J. Power Sources* 15 (1985) 179.
32. G. Oriji, Y. Katayama, T. Miura, *J. Power Sources* 139 (2005) 321.

33. A.J. Bard, L.R. Faulkner, *Electrochemical Methods: Fundamentals and Applications*, Wiley, New York (2001).
34. C. Gao, N. Wang, S. Peng, S. Liu, Y. Lei, X. Liang, S. Zeng, H. Zi, *Electrochim. Acta* 88 (2013) 193.
35. G. Wei, C. Jia, J. Liu, C. Yan, *J. Power Sources* 220 (2012) 185.
36. K. Gong, F. Xu, J.B. Grunewald, X. Ma, Y. Zhao, S. Gu, Y. Yan, *ACS Energy Letters* 1 (2016) 89.

© 2017 The Authors. Published by ESG (www.electrochemsci.org). This article is an open access article distributed under the terms and conditions of the Creative Commons Attribution license (<http://creativecommons.org/licenses/by/4.0/>).